Ab initio investigation of the structural and unusual electronic properties of α-CuSe (klockmannite)

Ali Reza Shojaei[a)b)†], Zahra Nourbakhsh[a)], Aminollah Vaez[a)], and Mohammad Dehghani[a)]

[a)] *Physics Department, Faculty of Science, University of Isfahan*, 81746-73441 *Isfahan, Iran*
[b)] *Physics Department, Technical and Vocational University-Mohajer Center*, 81645-315 *Isfahan, Iran*

(Received 21 May 2013; revised manuscript received 17 June 2013)

In this article, a computational analysis has been performed on the structural properties and predominantly on the electronic properties of the α-CuSe (klockmannite) using density functional theory. The studies in this work show that the best structural results, in comparison to the experimental values, belong to the PBEsol-GGA and WC-GGA functionals. However, the best results for the bulk modulus and density of states (DOSs) are related to the local density approximation (LDA) functional. Through utilized approaches, the LDA is chosen to investigate the electronic structure. The results of the electronic properties and geometric optimization of α-CuSe respectively show that this compound is conductive and non-magnetic. The curvatures of the energy bands crossing the Fermi level explicitly reveal that major charge carriers in CuSe are holes, whose density is estimated to be 0.86×10^{22} hole/cm^3. In particular, the Fermi surfaces in the first Brillouin zone demonstrate interplane conductivity between (001) planes. Moreover, the charge carriers among them are electrons and holes simultaneously. The conductivity in CuSe is mainly due to the hybridization between the d orbitals of Cu atoms and the p orbitals of Se atoms. The former orbitals have the dual nature of localization and itinerancy.

Keywords: klockmannite, α-CuSe, structural properties, electronic properties

PACS: 71.20.−b, 71.15.Mb, 71.18.+y, 72.80.−r **DOI:** 10.1088/1674-1056/22/12/127102

1. Introduction

Research on semiconductor materials is one of the appealing topics in condensed matter physics. During years of research, many compounds have been empirically investigated. Among them, copper selenide (CuSe) is a compound in which a variety of interesting effects were observed. The CuSe is a slate gray mineral usually known as klockmannite.[1] During the past few decades, various experimental efforts on natural and synthetic mineral klockmannite have been made to determine the structural properties of this compound.[1–13] These efforts determined the crystal structure of CuSe in three structural phases: α, β, and γ. In the early years of research on this compound, Earley[1] and Berry[2] demonstrated that the crystal structure of klockmannite (CuSe) is similar to covellite (CuS) with the space group $P6_3/mmc$ ($Z=6$) and that their compositions are the same. Nevertheless, unlike covellite, klockmannite has a hexagonal superstructure.[3,4] It undergoes two phase transitions with thermal changes. However, the reported transition temperatures in these efforts are different from each other. This was reviewed in Milman's work.[14] It seems that to some extent, these differences could be due to the dependence of the results on utilized synthetic samples in the experiments because the nature of klockmannite is unsuitable for the preparation of its single crystal.[2] According to the data reported by Stolen,[13] the crystal structure of α-phase is hexagonal at room temperature (Fig. 1) and it undergoes a transition to a β orthorhombic structure at 327 K. The second-order transition occurs with the further increase in temperature between the β phase and the γ hexagonal phase at 410 K. The γ hexagonal has different lattice constants from the initial α hexagonal.[14] The γ crystal structure is stable up to almost 652.7 K.[13] Above this temperature, the γ-CuSe decomposes into $Cu_{2-x}Se_x$ and a liquid rich in selenium.[5,10]

Among the computational[14] and experimental[15] studies carried out on klockmannite, there is a major difference for values of the bulk modulus and its pressure derivative. In 1998, Peiris's experiments on the compression of klockmannite yielded 96.9 ± 5 GPa for the bulk modulus using the third-order Birch–Murnaghan equation of state (EOS) fit.[15] Thereafter, in 2002, the *ab initio* calculation performed on klockmannite by Milman yielded 69 GPa for the bulk modulus of α-CuSe by employing PW–GGA pseudopotential for the exchange–correlation functional.[14] This difference was significant. Hence, Milman reviewed Peiris's experimental values and fitted the experimental data again, then he suggested 72 GPa as the empirical amount. This difference is a challenge for the experimental values of the bulk modulus and its pressure derivative for the α-CuSe.

Among the studies performed on klockmannite, the known electronic properties of CuSe bulk are based on the results of the Hall-effect experiment, which indicated the p-type conductivity implicitly in α-CuSe[16] and the X-ray photoelectron spectroscopy (XPS) experiment that determined its electronic structure.[17] In recent years, research on this compound has focused more on the electronic and optical properties of its thin films.[18,19] In summary, we can refer to all the specific properties of klockmannite, such as the complex crystal structure, the interesting thermal behavior with an intermediate orthorhombic phase, the non-magnetic behavior, the metallic conduction and the p-type electrical carriers. Nonetheless, principles of these properties are still vague to some extent or unknown. In order to understand the CuSe behavior in the α phase and to provide reliable theoretical electronic struc-

†Corresponding author. E-mail: Ali.r.shojaei@gmail.com

© 2013 Chinese Physical Society and IOP Publishing Ltd

ture data, which are very important for using this material in opto-electronic devices, the aim of this paper is to conduct a comprehensive study on its electronic properties at the ground state as well as on its structural properties obtained by *ab initio* calculations based on the density functional theory. The calculations were only performed on the α phase, which is the most stable phase of CuSe crystal. The structural properties, density of states (DOSs), band structure and Fermi surface were also calculated.

In Section 2, the details of calculations are described in brief. In Section 3, our results are presented and discussed in comparison with the available experimental data and other theoretical results. In Section 4, the correlation and localization effects in 3d electrons of copper atoms are discussed. Finally, the main results and conclusions are summarized in Section 5.

2. Calculations details

All the calculations in this work were performed within the framework of the density functional theory (DFT)[20] using the full potential augmented plane waves plus the local orbitals (APW + lo) method implemented in the WIEN2k package.[21,22] To calculate the exchange–correlation functional, the generalized gradient approximation PBE–GGA,[23] PBEsol–GGA,[24] WC–GGA[25] and the local density approximation (LDA)[26] were used. The following parameters were used in our calculations: a mesh of 88 special k-points was taken in the irreducible wedge of the first Brillouin zone corresponding to the grids of $20 \times 20 \times 3$. The maximum of l for expanding the Kohn–Sham wave functions in terms of lattice harmonics inside atomic spheres was chosen to be $l_{\max} = 10$. In the interstitial region, the maximum value of the wave vector for expanding the wave functions in terms of plane waves was chosen to be $K_{\max} = 8/R_{\mathrm{MT}}$ (a.u.)$^{-1}$, where R_{MT} is the smallest muffin-tin radius in the unit cell. The muffin-tin radii were chosen 2.13 (a.u.) for both Cu and Se atoms. The charge density and the potential were expanded up to $G_{\max} = 14.5$ (Ry)$^{1/2}$. All these values were optimized in terms of the total energy. The separation energy between the core and the valence electrons has been considered to be -6.0 Ry. The core electrons were treated fully relativistically, but the valance electrons were treated in scalar and relativistically. In order to increase the accuracy of the results, spin–orbit coupling was considered in all calculations and optimizations. Since the α-CuSe is the most stable crystal phase, all calculations in this work have been made in this phase with the space group $P6_3/mmc$.

3. Results and discussion

3.1. Structural properties

The crystal structure of α-CuSe is modified in an anisotropic complex hexagonal with space group $P6_3/mmc$ ($Z = 6$) and lattice constants $a = 3.938$ Å and $c = 17.25$ Å (Fig. 1). In this structure, two Cu_I atoms are located in position $2d$: (1/3, 2/3, 1/4), two Se_I atoms in position $2c$: (2/3, 1/3, 1/4), four Cu_{II} atoms in position $4f$: (2/3, 1/3, Cu_z) and four Se_{II} atoms in position $4e$: (0, 0, Se_z).[2] This structure could be described as $CuSe_3$ triangles surrounded by $CuSe_4$ tetrahedral (Fig. 1). The structure provided an alternating structure with the alternation of $CuSe_4$–$CuSe_3$–$CuSe_4$ layers connected by covalent bonds between Se atoms of Cu_2Se_2 double layers (Fig. 1). As mentioned before, the low temperature structure of klockmannite (α-CuSe) has a hexagonal superstructure with dimensions $A = (13)^{1/2}a$, $C = c$, and $P6_3/m$ space group ($Z = 78$) related to the inexact positioning of some copper atoms in the hexagonal flat layers.[3,4]

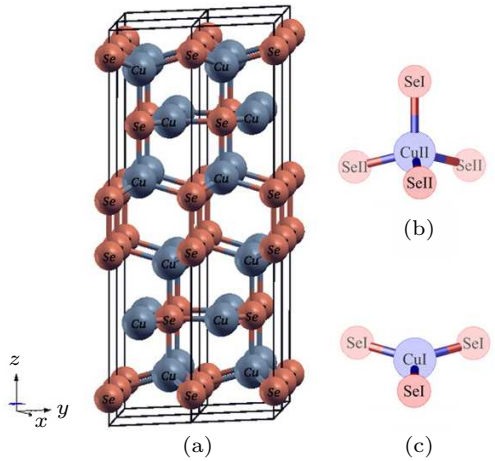


Fig. 1. (color online) (a) Crystal structure of α-CuSe and its structural details with neighboring atoms (b) $CuSe_4$ tetrahedral with Cu_{II} atoms (c) $CuSe_3$ flat triangles with Cu_I atoms.

In order to study the structural properties, the accuracy of the calculated lattice parameters has been considered as the criterion and the Peiris' results as references for experimental values. In order to determine the equilibrium lattice constants of CuSe in the α-phase, the total energy of CuSe in this phase with various unit cell volumes has been calculated using PBE–GGA, PBEsol–GGA, WC–GGA, and LDA approaches in both ferromagnetic and non-magnetic phases. For the structural optimization process, the volume and the c/a ratio are changed simultaneously using two-dimensional (2D)-optimized package under the Wien2k code. This package performs a 2D structure optimization for hexagonal or tetragonal space groups by generating a set of different structures from the viewpoint of volume and c/a ratio simultaneously. The forces acting on each atom are minimized to less than 1 mRy/a.u. for all structures before the optimization process. The calculated total energy versus volumes is fitted with the third order Murnaghan (MEOS) and Birch–Murnaghan (BMEOS) EOS. The obtained Figs. of optimization show that energy–volume curves in the ferromagnetic and non-magnetic phases are identical for all

approaches. Therefore, it could be concluded that α-CuSe is a non-magnetic compound. Table 1 shows the calculated lattice parameters, bulk modulus, its pressure derivative, and internal coordinate compared to experimental values as well as those of other works. As is evident from the results, unlike LDA, the lattice constants of PBE–GGA are much larger than the experimental values. Consequently, the equilibrium volume (V_0) of PBE–GGA has been calculated as being much larger than the others. This issue has a negative impact on calculating its bulk modulus because it depends directly on the inverse of the volume ($1/V_0$). It seems that the main reason for the difference between the PBE–GGA and PW–GGA bulk modulus in Milman's work with experimental values is the difference of the calculated V_0 for these two methods with the experimental V_0. Because all results of PBE–GGA are incompatible with the experimental values, it could be deduced that the PBE–GGA functional is unsuitable for calculating structural properties of α-CuSe. Although other modified versions of GGA, such as PBEsol–GGA and WC–GGA, give better values in quantitative agreement with the experimental values specially for lattice parameters, among these approaches, PBEsol–GGA and WC–GGA are the best candidates for the study of the α-CuSe structural properties with the lattice parameters criterion. However, the best value of the bulk modulus is obtained from LDA that is in good agreement with Peiris' experimental values. Since the experimental data are mostly obtained at room temperature and the calculated data are obtained under absolute zero temperature, it appears that a decrease in the calculated equilibrium volume is natural. If this issue is accepted as a fact, then one can claim that LDA values are very good for the bulk modulus and in good agreement with Peiris' values. In summary, the calculated values of the bulk modulus depend simultaneously on two main factors: the curve slope of energy–volume and the ratio of $1/V_0$. It seems that because the V_0 of LDA is smaller than the V_0 of the PBEsol–GGA or WC–GGA functionals, the LDA bulk modulus is larger than the other two.

Table 1. Calculated values of the lattice parameters, bulk modulus (B), and its pressure derivatives (B'), also the internal coordinates of atoms in comparison to the experimental values and those obtained in other works.

Approaches	Lattice parameters			BMEOS		MEOS		Internal coordinate	
	a/Å	c/Å	V_0/Å^3	B/Gpa	B'	B/Gpa	B'	Se_{zII}	Cu_{zII}
LDA	3.905	16.956	223.961	86.53	4.81	86.17	4.50	0.071	0.109
PBE–GGA	4.018	17.531	245.073	67.06	4.59	68.62	4.08	0.070	0.109
WC–GGA	3.951	17.183	232.325	78.57	4.69	79.30	4.27	0.070	0.109
PBEsol–GGA	3.947	17.167	231.650	78.64	4.69	79.27	4.28	0.070	0.108
PW–GGA[14]	3.975	17.355	237.481	69	5.1				
Revised values[14]				72	4.6				
Exp[2]	3.938	17.250	231.670	96.9 ± 5	4.1 ± 0.5			0.066	0.107

As a result of the values of PBEsol–GGA and WC–GGA as well as LDA, one could reject Milman's revised values because they are produced to be compatible with the PW–GGA results. However, our results, that are based on the full-potential method, reject the PW–GGA results, which are based on pseudo-potential methods. Hence, the criterion for the bulk modulus will be Peiris' values henceforth, unless a new investigation is carried out on compression of klockmannite with more accuracy and new values are reported for these quantities. Finally, we can claim that in this work, the calculated results of α-CuSe bulk modulus have improved by PBEsol–GGA and WC–GGA than PW–GGA as well as by LDA, which is in good agreement with the Peiris' values.

At the end of structural studies, again a full structural relaxation was performed with the criterion of 1 mRy/a.u. on the exerted forces using their calculated lattice constants for each approach. At this stage, the internal coordinates of atoms are specified and presented in Table 1. Whereas the forces are minimized in this construction, the electronic properties can be found by turning off the relaxations and driving the system to achieve self-consistency.

3.2. Electronic properties

3.2.1. Density of states and band structure

In this section, the electronic properties of this compound were initially calculated with all the above mentioned approaches. The results showed that all these approaches have almost the same behavior in electronic properties. However, among them, the LDA has the best agreement in total DOSs with the experimental data (Section 4). Hence, LDA is chosen to investigate the electronic properties. In order to study the electronic characteristics, the total and the partial DOSs of α-CuSe in the energy region from -6.5 eV to above Fermi energy are plotted in Fig. 2. The Fermi energy (E_f) is set at zero as a reference. Because the CuSe compound is non-magnetic, the DOSs are displayed in a non-spin polarized manner. As it is clear from Fig. 2(a), the value of total DOS (TDOS) at the Fermi level is non-zero, indicating that the compound is a conductor. In addition, the DOS for each of the four base atoms has a non-zero value on the Fermi energy (Fig. 2(b)). Hence, all atoms are involved in the conductivity. These contributions are mainly related to d orbitals of Cu atoms and p

orbitals of Se atoms (Figs. 2(c), 2(d), 2(e), and 2(f)). Other s and p orbitals of Cu atoms and s orbitals of Se atoms have a very small contribution in the DOS near the Fermi level. Figures 2(b) and 2(c) clearly show that the largest contribution of the total DOS near the Fermi level comes from Cu atoms. The conductivity in CuSe is due to the hybridization of neighboring atoms near the Fermi energy (Figs. 2(g), 2(h), and 2(i)). To discover which partial orbitals participated in the conduction, the partial DOSs (PDOS) are studied. Figures 2(j) to 2(m) indicate PDOSs of different Cu and Se atoms, which include the d orbitals of Cu_I and Cu_{II} as well as the p orbitals of Se_I and Se_{II}. As Figs. 2(j) and 2(k) illustrate, the d_{xy} and $d_{x^2y^2}$ orbitals of Cu_I atoms and the d_{xy}, d_{xz}, d_{yz}, and $d_{x^2y^2}$ orbitals of the Cu_{II} atoms cross the Fermi level. In addition, the p_x and p_y orbitals of Se atoms cross the Fermi level (Figs. 2(l) and 2(m)). Hence, these partial orbitals have considerable effects on the conductivity of this compound. However, other orbitals do not have a considerable role in conduction. Consequently, they are probably involved in bonding and are localized.

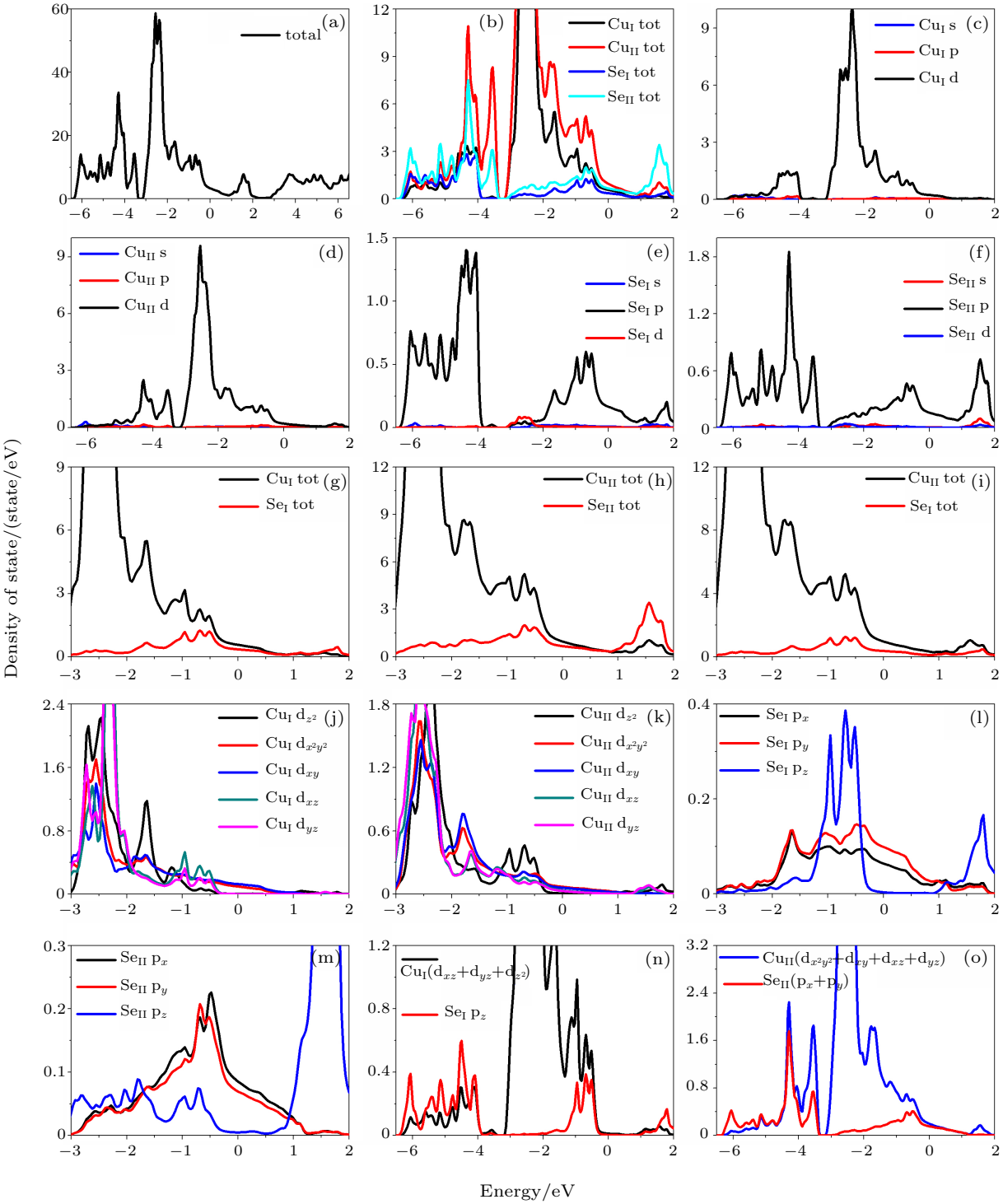


Fig. 2. (color online) Total DOS (TDOS) and partial DOSs (PDOSs) of α-CuSe, whose Fermi energy is set as zero.

Figures 2(n) and 2(o) demonstrate that different partial orbitals of Cu and Se atoms have a similar trend near the Fermi level, which is a consequence of the hybridization among them. It should be noted that as a general rule, two orbitals are hybrids, providing that their DOSs have the following conditions.

(i) Two neighboring atoms must be close together to the extent that their atomic orbitals can overlap effectively.

(ii) Two orbitals that are hybrids must have similar behavior in an energy range near the Fermi level. On the other hand, any similar trend of PDOS at the low energy range away from the Fermi level does not demonstrate hybridization.

(iii) Partial orbitals of two different atoms should be able to interact head to head or side by side. Thus, they can overlap and link together.

Regarding the points mentioned above, the hybridization of the orbitals in CuSe could be divided into two different kinds.

i) Hybridizations that occur near the Fermi level in the energy range $[-0.5, 0]$ eV and cause conductivity in this compound. These hybridizations occur between the neighboring Cu_I and Se_I atoms (Fig. 2(g)), neighboring Se_{II} and Cu_{II} atoms (Fig. 2(h)), and Cu_{II} and Se_I (Fig. 2(i)). They also occur between ($d_{x^2y^2}$, d_{xy}) orbitals of Cu_I atoms with (p_x, p_y) orbitals of Se_I atoms and between ($d_{x^2y^2}$, d_{xy}, d_{xz}, d_{yz}) orbitals of Cu_{II} atoms with (p_x, p_y) orbitals of Se_I and Se_{II} atoms.

ii) Hybridizations occur in the energy range $[-6, -0.5]$ eV. These hybridizations cause atomic bonds. This means that orbitals do not participate in the conduction and are localized. They occur for the following orbitals.

a) ($d_{xz} + d_{yz} + d_{z^2}$) orbitals of Cu_I atoms hybridized with p_z orbital of Se_I atoms. These atoms are adjacent in hexagonal flat layers (Fig. 1). As it is clear from Fig. 2(n), these orbitals have been localized and do not cross the Fermi level. According to the spatial orientation of these orbitals, they bond together side by side diagonally. Hence, the formation of a delta covalent bond (δ) between these atoms is possible.

b) The p_z orbitals of Se_{II} atoms hybridized together head to head leading to the formation of a sigma covalent bond (σ) between these atoms.

c) Figure 2(o) shows ($d_{x^2y^2} + d_{xy} + d_{xz} + d_{yz}$) orbitals of the Cu_{II} atoms with the (p_x, p_y) orbitals of Se_{II} atoms in the range $[-6, 0]$ eV. As it is evident from this Fig., PDOSs have a similar trend in most areas. Hence, their hybridization is possible. Due to a lack of sufficient evidence, determining the type of bond between Cu_{II} and Se_{II} atoms requires more calculations and careful considerations.

Figure 3 shows the band structure of CuSe with LDA along different high-symmetry directions in the first Brillouin zone of the hexagonal lattice. As it is clear from this Fig., near the Fermi energy, the energy bands are divided into two parts. The first is from -6.4 eV to -3.4 eV and the second is from -3.1 eV to above the Fermi level. These two sections have an internal energy gap of about 0.3 eV. The bands of the second section cross the Fermi level, causing the conductivity in this compound. As is evident from this Fig., eight energy bands cross the Fermi level. These eight bands correspond to bands numbered 93 to 100, in which there are 14 electrons (Table 2). The occupation numbers of electrons and holes (E_{num} and H_{num}) in these bands are presented in Table 2. The E_{num} shows that these eight bands have different occupation numbers and E_{num} decreases with the increase in the bands number. The occupation numbers of bands crossing the Fermi level demonstrate the numbers of electrons and holes in the Fermi surface. Because all atoms in the compound participate in conduction, they contribute to these eight bands. Nevertheless, the d orbitals of Cu and the p orbitals of Se have more of a contribution to these bands. Slightly lower, in the energy range of -3.0 eV to -2.0 eV, the energy bands are almost flat; hence, the densities of states in this energy region are highly degenerate. These energy bands are mainly related to the d orbitals of Cu atoms; the effective mass of the electrons is much larger.

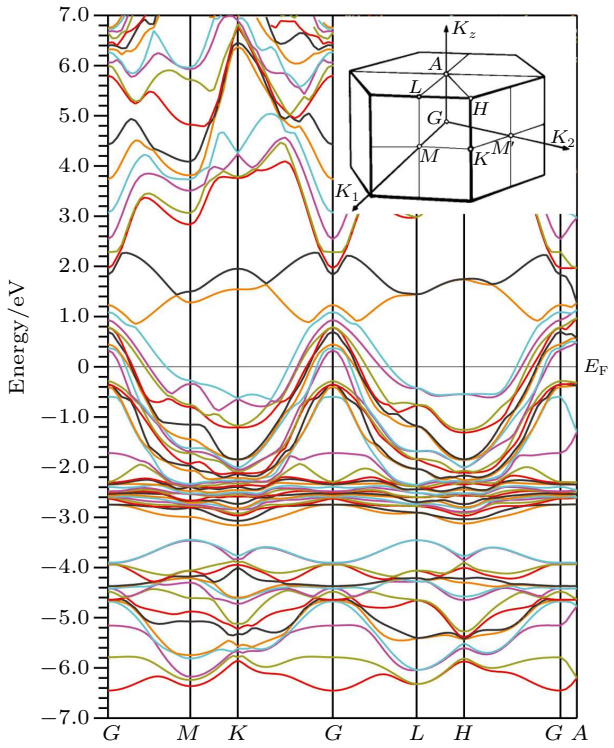


Fig. 3. (color online) The band structure of CuSe with LDA and the first Brillouin zone of the hexagonal lattice.

As is obvious from the shape of Fermi bands, the curvature of energy bands crossing the Fermi level is downward; consequently, the charge carriers have a negative effective mass. This means that the conductivity in this compound is caused by holes compatible with the experimental results.[16,17] According to Table 2, there are 14 electrons in eight bands, so the number of holes is nearly two holes per unit cell. Hence, the hole's density is estimated to be 0.86×10^{22} hole/cm^3. In addition, bands crossing the Fermi level in the vicinity of the G point are related to the (100),

(110), (011), and (111) crystal planes. Thus, there is conductivity between each of these crystal planes, but in the direction of G to A, i.e. the normal direction of (001) crystal planes set, the bands are above the Fermi level. Therefore, to clarify the interplane conductivity between (001) planes, the Fermi surface of CuSe is investigated in the next section.

Table 2. Electrons and holes occupation numbers ($E_{\rm num}$ and $H_{\rm num}$) in valence bands crossing the Fermi level.

Valence bands number	Minimum energy of valence bands/eV	Maximum energy of valence bands/eV	$E_{\rm num}$	$H_{\rm num}$
93	−2.024	0.288	1.952	0.048
94	−1.983	0.356	1.928	0.072
95	−1.861	0.410	1.872	0.128
96	−1.847	0.533	1.849	0.151
97	−1.344	0.641	1.796	0.204
98	−1.260	0.723	1.720	0.280
99	−0.963	0.859	1.530	0.470
100	−0.746	0.886	1.353	0.647
Total occupation number of valence bands			14.000	2.000

3.2.2. Fermi surface of CuSe

Figure 4 displays the calculated Fermi surface of CuSe with the LDA method. These surfaces consist of eight quasi-cylindrical sheets, all located coaxially around the direction of G to A (Fig. 3). Each of these surfaces corresponds to one of the energy bands that crosses the Fermi level from number 93 to 100. Radii of these quasi-cylindrical sheets increase with the increase in bands numbers. The formation of these surfaces is due to the p–d hybridization between Se and Cu neighboring atoms on the Fermi energy. It should be noted that the total volume surrounded by each sheet, related to one band, depends only on the number of charge carriers in its band. Thus, the ratio of the surrounding volume of each sheet to the volume of the first Brillouin zone is equal to the amount of charge carriers in the band. As it is apparent from Table 2, the electron occupation numbers of the bands in CuSe are in contradiction to this point. Obviously, the lower bands have larger electron occupation numbers. However, as shown in Fig. 4, the lower bands have lower volumes in the first Brillouin zone. This contradiction is due to the fact that the main charge carriers in the compound are holes. For example, the volume of the sheet related to band number 100 is nearly one third of the first Brillouin zone volume, which is compatible with the hole occupation number in this band (Table 2). Therefore, comparing the occupation numbers of the bands with the volume of the Fermi surface, one can recognize the type of charge carriers in the compound. This result is also compatible with the curvature of bands near the Fermi level (Fig. 3).

As mentioned in the previous section, the energy bands along the G to A direction are above the Fermi level. Hence, to investigate the conductivity between the (001) planes set, we have considered the shape of sheets along the G to A direction. Figure 4 shows the Fermi surfaces creating open circuits around this direction. The Fermi surfaces do not cross the G to A direction, but they cross other directions parallel to the G to A direction. Hence, the interplane conductivity is due to both electrons and holes simultaneously as a result of the open circuits around the (001) direction. This simultaneity of carriers arises from the smaller contribution of the electrons on the Fermi level in the z direction rather than in the other directions.

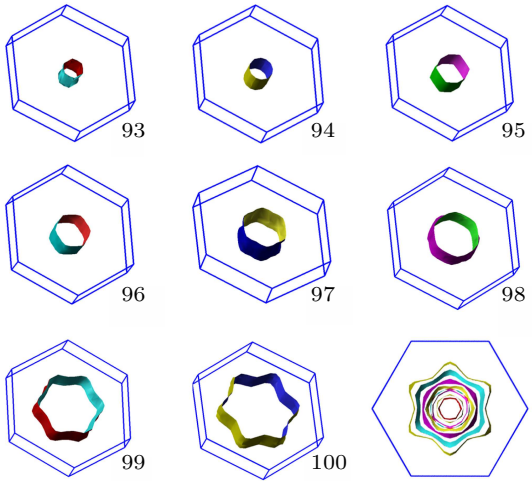


Fig. 4. (color online) Fermi surfaces of the CuSe with LDA in the first Brillouin zone of the hexagonal lattice for the bands 93 to 100; all surfaces are quasi coaxially cylindrical around the direction of G to A.

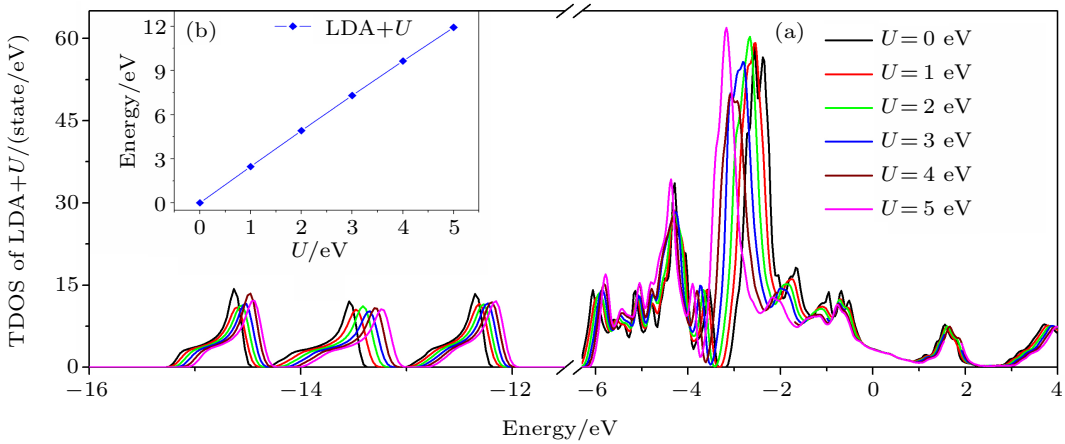


Fig. 5. (color online) (a) Total DOS for several LDA + U approximations with $U = 0$ to 5 eV. (b) Changing the total energy of the system for different Hubbard parameters in the LDA + U method, the total energy of LDA is set as zero energy as: $E = E_{\rm LDA+U} - E_{\rm LDA}$.

4. Correlation and localization effects in 3d electrons of Cu atoms

In the last section, we mentioned that the 3d-Cu orbitals in CuSe have the main contribution in the DOS near the Fermi level and in the electrical conductivity. Hence, in this section, we investigate the correlation effects on these orbitals and on the compound's conductivity. In order to study these effects, the Hubbard correction has been used. Therefore, the electronic structure of the compound, with the LDA + U method, is calculated using different values of Hubbard parameters, U, from $U = 1$ eV to 5 eV. In Fig. 5(a), the total DOSs with the LDA and the LDA + U method with different values of U are presented. As is evident from this Fig., by applying the Hubbard correction on 3d orbitals of Cu atoms, the main peaks of the DOSs are pushed toward the inner layers. Nevertheless, the amount of DOSs have not changed near the Fermi level. Hence, it could be concluded that the conductivity in CuSe is not sensitive to the correlated effects for all the selected values of U. Whereas by considering the correlation effects on orbitals of 3d-Cu, these orbitals recede from the Fermi level and are placed in lower energies; it is expected that the energy level of the system decreases. To examine this issue, in Fig. 5(b), the total energy of the system is calculated with different Hubbard parameters in the LDA + U method. From Fig. 5(b), it is clear that contrary to our expectation, the total energy of the system increases with the increase in the Hubbard parameter near-linearly. Since, among these energies, the least energy is related to LDA, it could be deduced as an opinion that 3d orbitals of Cu atoms in this compound are not correlated, or the correlation effects in these orbitals are very little. In other words, probably CuSe is not a correlated compound owing to the fact that the strong correlation effects in materials are generally more important in f-orbitals than d-orbitals. Especially in CuSe, that 3d-Cu orbitals are almost filled. From a different point of view, it could be an appropriate opinion if the peaks of calculated and experimental DOSs have acceptable agreement together. In order to investigate this opinion, the calculated and experimental[17] DOSs are compared in Fig. 6. The experimental DOS is extracted from Folmer's work, which was done on experimental DOS of some copper selenide compounds. In this work, the main peak of the CuSe experimental DOS was reported about 3 eV under the Fermi level.[17] Hence, to compare the exact value of its peak with this work, the horizontal axis of the experimental DOS curve is rescaled with the computer. The exact position of the experimental and calculated peak of DOSs were obtained about 2.61 eV and 2.56 eV under the Fermi level, respectively. These results are in good quantitative agreement together; hence, this opinion is illustrated by another method. Moreover, it could be deduced that LDA is a good approximation to describe the electronic structure of this compound. Because of the extension of the d-orbitals of Cu atoms up to the Fermi level as well as their main contribution in the DOS near the Fermi level, it could be deduced that these orbitals have the dual property of localization and itinerancy. Thus, a successful description of the electronic structure of α-CuSe by LDA is very appealing because this simple approach is based on the behavior of the uniform electron gas. We believe that there are mainly two reasons for duality in the nature of 3d-electrons of Cu atoms near the Fermi energy.

(I) According to experimental results,[17] the ionization numbers of Cu nucleons in α-CuSe are Cu^{1+}. Since the electronic configuration of the copper atoms is $[Ar]3d^{10}4s^{1}$, the 3d orbitals of Cu atoms in CuSe are almost filled. In addition, our calculations show that the ionization numbers of Cu nucleons are fewer than one positive charge. Hence, a small charge on copper nucleons has a minor effect on the contraction of 3d orbitals and their localization.

(II) The second reason, more important than the first one, is based on the mechanism of hybridizations near the Fermi level (Subsubsection 3.2.1). The p–d hybridizations near the Fermi energy cause conductivity between Cu and Se atoms. This hybridization is the consequence of the attraction of partial-empty p orbitals of Se atoms on d orbitals of Cu atoms. Thus, these orbitals are extensive up to the Fermi level and find a dual nature between localized and itinerant states.

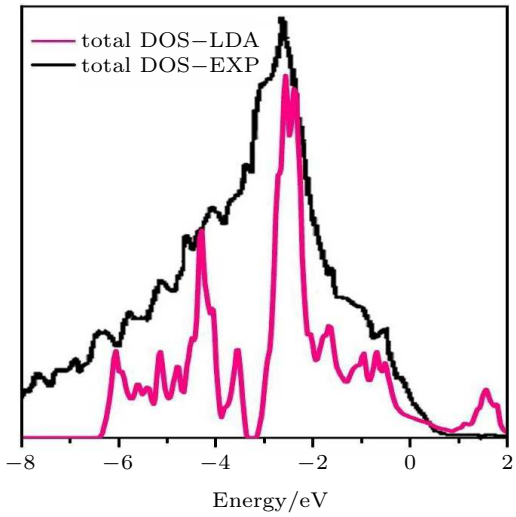


Fig. 6. (color online) The calculated and experimental[17] DOSs are compared and the Fermi energy is set as zero energy.

5. Conclusions

In this work, a computational investigation on the structural and predominantly on the electronic properties of the α-phase of klockmannite (α-CuSe) has been performed using density functional theory. The generalized gradient approximations PBE–GGA, PBEsol–GGA, WC–GGA, and also the local density approximation (LDA) have been used to calculate the structural properties of this compound. Our studies show that the PBE–GGA functional yields incompatible results with experimental values for the structural properties of α-CuSe. It seems that this difference in results could proceed from the weakness of PBE–GGA and probably PW–GGA in

Milman's work for calculating the minimum volume, V_0, of α-CuSe. Hence, it is deduced that the PBE–GGA functional is not suitable for calculating the structural properties of α-CuSe. Among these approaches, the consequences of PBEsol–GGA and WC–GGA are better than the LDA approach to calculate the structural properties when the criterion is considered as accurate as the calculated lattice parameters. Nevertheless, the best value for the bulk modulus is related to the LDA functional, which is in good agreement with the experimental value.

In the initial studies of electronic properties, the LDA showed that it has better DOS results for α-CuSe with respect to the experimental results. Therefore, the LDA is chosen to investigate the electronic structure. The results of electronic properties and geometric optimization of α-CuSe, respectively demonstrated that this compound is conductive and non-magnetic. The curvature of energy bands crossing the Fermi level illustrates that the major charge carriers in CuSe are holes, whose density is estimated to be 0.86×10^{22} hole/cm^3. The bands around the G point, crossing the Fermi energy, are related to the (100), (110), (011), and (111) planes set. These bands show that there is conductivity among them. In particular, the Fermi surfaces in the first Brillouin zone demonstrate the interplane conductivity between (001) planes. Moreover, the charge carriers are electrons and holes between the planes simultaneously as a result of fewer Fermi electrons in the (001) direction in comparison to other directions. The DOSs near the Fermi energy are mainly because of the d orbitals of Cu atoms and p orbitals of Se atoms. Also, the conductivity in CuSe is mainly due to the hybridization between the d orbitals of Cu atoms and the p orbitals of Se atoms. The d orbitals of Cu atoms in the energy range of -3.0 eV to -2.0 eV are highly localized, but they are extended up to the Fermi level. These properties indicate the dual nature of the localization and itinerancy in these electrons. The itinerant feature of d orbitals is mainly due to the attraction of partially-empty p orbitals of Se atoms on d orbitals of Cu atoms.

Acknowledgment

This work has been performed based on research project number 2054361 in the University of Isfahan (UI), Isfahan, Iran.

References

[1] Earley J W 1949 *Am. Mineral* **34** 435
[2] Berry L G 1954 *Am. Mineral* **39** 504
[3] Taylor C A and Underwood F A 1960 *Acta Crystallogr.* **13** 361
[4] Lippmann F 1962 *Neues Jahrbuch Mineral Monatsh* 99
[5] Heyding R D 1966 *Can. J. Chem.* **44** 1233
[6] Elliott J A, Bicknell J A and Collinge R G 1969 *Acta Crystallogr., Sect. B* **25** 2420
[7] Elliott J A, Bicknell J A and Collinge R G 1969 *Acta Crystallographica B* **25** 2420
[8] Stevels A L N 1969 *Philips Research Reports Supplement* **9** 38
[9] Stevels A L N and Jellinek F 1971 *J. Phys. Chem.* **111** 273
[10] Heyding R D and Murray R M 1976 *Can. J. Chem.* **54** 841
[11] Brun G, Tedenac J C and Maurin M 1982 *Mater. Res. Bull.* **17** 379
[12] Nozaki H, Shibata K, Onoda M, Yukino K and Ishii M 1994 *Mater. Res. Bull.* **29** 203
[13] Stolen S, Fjellvg H, Grnvold F, Sipowska J T and Westrum J E F 1996 *J. Chem. Thermodyn.* **28** 753
[14] Milman V 2002 *Acta Crystallogr., Sect. B* **58** 437
[15] Peiris S M, Pearson T T and Heinz D L 1998 *J. Chem. Phys.* **109** 634
[16] Ogorelec Z and Selinger O 1971 *J. Mater. Sci.* **6** 136
[17] Folmer J C W and Jellinek F J 1980 *J. Less-Common Metals* **76** 153
[18] Pejova B and Grozdanov I 2001 *J. Solid State Chem.* **158** 49
[19] Gosavi S R, Deshpande N G, Gudage Y G and Sharma R 2008 *J. Alloys Compd.* **448** 344
[20] Hohenberg P and Kohn W 1964 *Phys. Rev. B* **136** 864
[21] Madsen G K H, Blaha P, Schwarz K, Sjostedt E and Nordstrm L 2001 *Phys. Rev. B* **64** 195134
[22] Blaha P, Schwarz K, Madsen G K H, Kvasnicka D, Luitz J and Schwarz K 2010 *WIEN2K, An Augmented Plane Waves + Local Orbitals Program for Calculating Crystal Properties* (Austria: Vienna University of Technology)
[23] Perdew J P, Burke K and Wang Y 1996 *Phys. Rev. B* **54** 16533
[24] Perdew J P, Ruzsinszky A, Csonka G B I, Vydrov O A, Scuseria G E, Constantin L A, Zhou X and Burke K 2008 *Phys. Rev. Lett.* **100** 136406
[25] Wu Z and Cohen R E 2006 *Phys. Rev. B* **73** 235116
[26] Perdew J P, Chevary J A, Vosko S H, Jackson K A, Pederson M R, Singh D J and Fiolhais C 1992 *Phys. Rev. B* **46** 6671